

## Stellar Populations in the Central Galaxies of Fossil Groups

Habib G. Khosroshahi<sup>1</sup> · Louisa A. Nolan<sup>2</sup>

<sup>1</sup> School of Astronomy, Institute for Research in Fundamental Sciences (IPM), PO Box 19395-5531, Tehran, Iran; email: [habib@ipm.ir](mailto:habib@ipm.ir)

<sup>2</sup> School of Physics and Astronomy, The University of Birmingham, Birmingham B15 2TT, UK

**Abstract.** It is inferred from the symmetrical and luminous X-ray emission of fossil groups that they are mature, relaxed galaxy systems. Cosmological simulations and observations focusing on their dark halo and inter-galactic medium properties confirm their early formation. Recent photometric observations suggest that, unlike the majority of non-fossil brightest group galaxies (BGGs), the central early-type galaxies in fossil groups do not have boxy isophotes, and are therefore likely to have formed in non-equal-mass, gas-rich galaxy-galaxy mergers.

Although the isophotal shapes of early-types can be used to infer the nature of the parent galaxies of their most recent mergers, detailed star-formation histories of the galaxies are also needed, in order to uncover the epoch of these mergers and the differences in the physical processes which produce fossil groups rather than ‘normal’ galaxy groups. In this study, we use a powerful long-baseline (UV-optical), multi-component, stellar population fitting technique to disentangle the star-formation history of the dominant central giant elliptical galaxy in a sample of five fossil groups, and compare this with a control sample of non-fossil BGGs, in an attempt to fully understand their merger histories. Our technique allows us to identify multiple epochs of star formation in a single galaxy, and constrain the metallicities of the constituent stellar populations. Resolving the populations in this way gives us a much clearer picture of galaxies’ histories than simply using the mean age / metallicity of total stellar populations recovered by more conventional techniques using absorption line strengths.

We find that i) the dominant stellar components in both galaxy samples are old ( $> 10$  Gyr), metal-rich ( $\geq$  solar) and statistically indistinguishable in terms of their ages, metallicities and relative mass fractions; ii) the ages of the secondary, younger stellar components are also statistically indistinguishable between the two samples; iii) the central fossil galaxies have secondary stellar components which have significantly lower metallicities than the corresponding stellar populations in the BGG sample.

In a gas-rich merger, dissipation dilutes the previously-enriched gas in the central regions of the parent galaxies with gas which has not been metal-enriched, lowering the metallicity of the stars produced. Hence, we conclude that the central fossil galaxies are the products of early and exceptionally gas-rich mergers, which leaves them with lower metallicities in their most recent merger-induced stellar populations than their BGG counterparts. In contrast, although the last starburst-inducing merger of the ‘normal’ BGGs occurred at the same epoch as that of the fossil BGGs, they have undergone a subsequent dissipation-less merger, leaving them in the present day with boxy isophotes and more disturbed x-ray emission, but no further significant star formation.

*Keywords:* ISM: molecules, ISM: structure, instabilities

## 1 Introduction

Most galaxy groups and clusters have a luminous elliptical galaxy which resides at the centre of the gravitational potential of the system. It is generally accepted that these galaxies have acquired the majority of their mass via galaxy-galaxy mergers [1]. This is confirmed by later simulations [2, 3, 4], although the precise nature of such mergers is still debated, for example the relationship between the morphology of the merging galaxies and the merger product [5, 6].

An interesting class of galaxy groups known as ‘fossil groups’ have been at the centre of recent studies [7, 8, 9, 10]. It is believed that these are the end product of galaxy mergers within a group, and as such, they should not have undergone any recent major mergers. Hence, they represent simple laboratories in which to test merger scenarios. Fossils are defined as galaxy groups, or clusters, with an X-ray luminosity of at least  $10^{42} \text{ erg/sec}$  and a large luminosity gap ( $\geq 2$  magnitude) between the two brightest galaxy in the system. This also means that typical luminosity galaxies ( $L^*$ ) galaxies are absent in the majority of the fossils, arguably as a result of multiple mergers of these galaxies within the group halo [11].

Fossils also show interesting properties in their inter-galactic medium (IGM). They have highly symmetric X-ray emission, which indicates the absence of recent group mergers. They are also outliers in some X-ray scaling relations. For instance, they are over luminous in X-ray for a given optical luminosity compared with ‘normal’ groups, and they have more concentrated dark matter halos [8]. These characteristics point to an early formation epoch for fossil groups. The study of fossils in the cosmological simulations [12] especially the recent detailed study of fossils in the Millennium Simulations by Dariush et al [13, 14] show that they assemble most of their mass earlier than non-fossils which have the same masses at the current epoch.

Galaxy groups usually have diverse properties [15, 16]. These are mainly attributed to their rapid evolution and recent formations [17] as the old groups usually don’t survive in the hierarchical structure formation. Given the absence of recent group mergers in fossil groups and their early formation epoch, they are ideal environments to study the formation and evolution of galaxies, especially the formation of giant elliptical galaxies in mature halos. The central galaxies in fossils are at least as luminous as those in non-fossil groups and clusters [18, 19], however study of Khosroshahi et al [20] presented clues that isophotal shapes of those in fossil groups are non-boxy in contrast to the majority of massive ellipticals. This is later explored by Smith et al [9]. Numerical studies of galaxy mergers suggest that boxy isophotes are produced either in equal mass mergers, or mergers between bulge-dominated systems, regardless of mass ratio [6]. Central fossil galaxies are therefore likely to be the result of gas-rich mergers.

Probing the morphology of central fossil galaxies provides the first constraint on their merger and interaction history. Exploring their stellar populations allows us to further understand the nature of their merger history. Studies of the stellar populations of early-type galaxies have been carried out by, for example, Trager et al [21], Terlevich & Forbes [22] and van Zee et al [23]. These used absorption line strengths to extract luminosity-weighted *mean* ages and metallicities for the stellar populations of early-type galaxies. However, our new approach, fitting multi-component stellar population models to long-baseline (ultraviolet-optical) spectra, can uncover a more detailed star-formation history. The long-baseline spectra contain sufficient data to lift the age-metallicity degeneracy and also to disentangle multiple stellar components [24]. Hence, we can know the epoch of the last major merger-induced starburst more accurately than when fitting to individual spectral lines, which give us only an upper limit to the age of the last (presumably merger-induced) starburst in these galaxies.

In this spirit we study a sample of five central fossil galaxies, which although it is small, is still the largest sample available. We explore the nature and epoch of the last major interactions/mergers they have experienced, and compare with a control sample of seven brightest group galaxies. Section two describes the data and the observations. A short description of the method and the results are provided in section 3. Section 4 contains a summary and discussion of the results. We adopt a cosmology with  $H_0 = 70 \text{ km s}^{-1} \text{ Mpc}^{-1}$  and  $\Omega_m = 0.3$  with cosmological constant  $\Omega_\Lambda = 0.7$  throughout.

## 2 The Sample

This study uses a sample of five giant elliptical galaxies dominating fossil groups and seven BGGs in non-fossil groups, all with long-baseline optical spectra.

The spectroscopic observations of the fossil sample were performed using a multi-slit spectrograph on the KPNO 4-m telescope on the 2000 March 11th. The Ritchey-Cretien spectrograph and KPC-10  $\text{\AA}$  grating gave a dispersion of  $2.75 \text{ \AA pixel}^{-1}$  over 3800-3850  $\text{\AA}$  and with 1.8-arcsec slitlets, a resolution of 6  $\text{\AA}$  [full width at half-maximum (FWHM)] was achieved. Risley prisms compensated for atmospheric dispersion. Spectra were obtained through three slitmasks, with typically an hour exposure on each. The spectroscopic data were reduced and analysed in the standard way using IRAF.

The brightest group galaxy (BGG) sample was selected from the well-studied groups in the Group Evolution Multi-wavelength Study, GEMS [25]. The groups in which the BGGs reside have a range of X-ray properties [16], and were selected for the archived availability of their ultraviolet-to-near-infrared spectra. Table 1 lists the sources for the spectra. The BGG names are the same as the names of their host groups.

For both the BGGs and the fossil BGGs, it is the central  $\sim$  one fifth of the effective radius ( $r_e$ ) of the galaxies which was observed.

We compared the properties of the BGG sample, namely the  $K_s$ -band luminosity, with a much larger sample of BGGs listed by Ellis & O'Sullivan [26] and noted that our sample has a mean solar  $K_s$ -luminosity of 11.1 with a standard deviation of 0.2 while the same quantities for the BGGs in the Ellis & O'Sullivan [26] sample are 11.3 and 0.3, respectively. Our fossil central galaxies are in general more luminous (mean  $K_s$ -luminosity of 11.7 and standard deviation of 0.4). As we argue below, this should strengthen our conclusions rather than the opposite.

## 3 The Analysis and Results

### 3.1 The Star-Formation History

To determine the star-formation history of the fossil and brightest group galaxies, we use the powerful long-baseline two-component stellar population fitting technique, as described in detail in Nolan et al [24]. We use the Bruzual & Charlot [27] single stellar population synthesis models, and note that our results in Nolan et al (2007) were robust to choice of model. The Bruzual & Charlot [27] models have ages ranging from 0.01 – 14 Gyr. Solar metallicity ( $Z_\odot$ ) is 0.02, and the available metallicities are: 0.02, 0.2, 0.4, 1.0 and 2.5  $Z_\odot$ . The age, metallicity and relative stellar mass fraction of each component were allowed to vary as free parameters in the fitting process. The best-fitting parameters of the two stellar populations were recovered via  $\chi^2$  minimisation. As in Nolan et al [24], we fit the various spectral sections (ultraviolet, optical, near-infrared) for each galaxy simultaneously, but with the relative normalisations allowed to float independently, to compensate for any deviations

Table 1: Archive sources of the spectra for the non-fossil BGGs. The Bica & Alloin data are available at <ftp://cdsarc.u-strasbg.fr/cats/III/219/galaxy/>, and those for NGC 1052 and NGC 1407 are available at [http://www.stsci.edu/ftp/catalogs/nearby\\_gal/sed.html](http://www.stsci.edu/ftp/catalogs/nearby_gal/sed.html).

object	source	wavelength / Å
NGC 1052	IUE Newly Extracted Spectra	2500 – 3200
	Storchi-Bergmann, Calzetti & Kinney unpublished	3200 – 7500
NGC 1407	Storchi-Bergmann, Calzetti & Kinney unpublished	3200 – 7500
IC 1459	Bica & Alloin, unpublished	3100 – 5400
	Bica & Alloin, 1987a	3800 – 7500
NGC 3557	Bica & Alloin, 1987a	3800 – 7500
	Bica & Alloin, 1987b	6400 – 8500
NGC 3923	Bica & Alloin, unpublished	3100 – 5400
	Bica & Alloin, 1987a	3800 – 7500
	Bica & Alloin, unpublished	3100 – 5400
NGC 4697	Bica & Alloin, unpublished	3100 – 5400
	Bica & Alloin, 1987a	3800 – 7500
	Bica & Alloin, 1987b	6400 – 8500
NGC 7144	Bica & Alloin, unpublished	3100 – 5400
	Bica & Alloin, 1987a	3800 – 7500
	Bica & Alloin, 1987b	6400 – 8500

in the flux calibration. Some long single sections have been split into two to compensate for any potential flux deviations across the broad wavelength range. Sky lines and emission lines are masked out of the fit. We use two components rather than three or more as we expect the bulk of the stars in most early-type galaxies to be represented by two components [28], and increasing the number of components rapidly becomes computationally expensive for diminishing returns.

Figure 1 presents the best-fitting parameters recovered from the two-component fitting. The galaxy spectra, with the best-fitting two-component models overlaid, are shown in Figures 2 and 3. In Figure 1, it can be seen that, although the dominant populations in both samples are old and metal-rich ( $\geq Z_{\odot}$ ), the younger, secondary, stellar populations are generally of a lower metallicity in the fossil population than for the BGGs. The statistics presented in Table 2 confirm this. The distributions of the ages, metallicities and relative mass fractions of the dominant stellar populations in the two samples are indistinguishable from each other, and the Kolmogorov-Smirnov probabilities suggest that it is highly likely that they are drawn from the same population. However, for the second components, the metallicity distributions are significantly different, although the ages are not. The Kolmogorov-Smirnov probability that the metallicities are drawn from the same distribution is less than 20%, and the BGG populations have a mean metallicity more than three times that of the fossils.

### 3.2 Photometric Analysis

The photometric properties of our sample of central fossil galaxies, i.e. their isophotal shapes and radial surface brightness distributions, were presented in Khosroshahi, Jones & Ponman [20]. The results were based deep R-band and  $K_s$ -band photometry of the sample observed

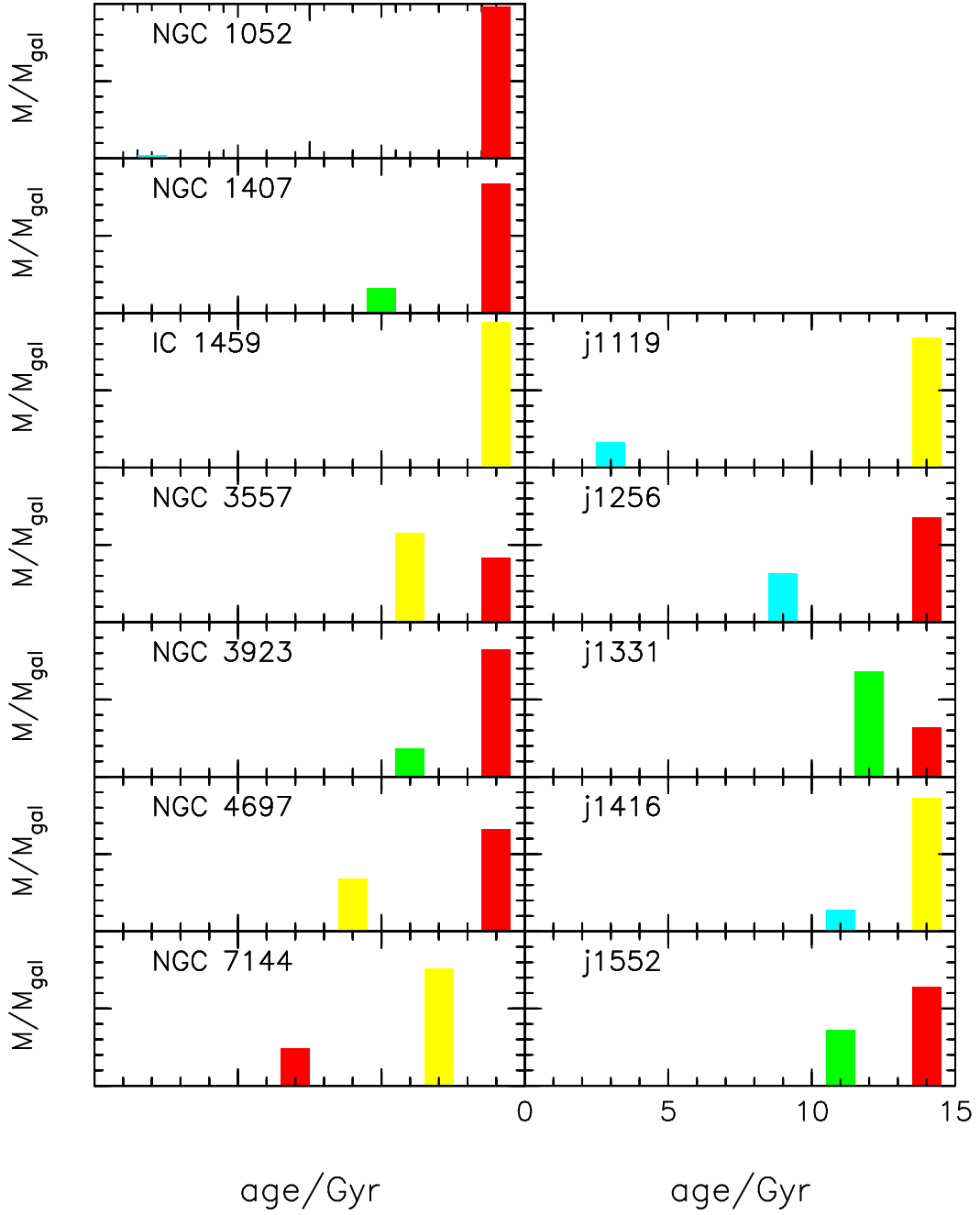


Figure 1: The best fitting parameters recovered from the two-component stellar population model fitting to the long-baseline spectra of the brightest group (**left**) and fossil galaxy (**right**) samples. The height of the histograms represent the fractional stellar mass of each component, and the colours represent the recovered metallicities: **red:**  $5 Z_{\odot}$ ; **yellow:**  $Z_{\odot}$ ; **green:**  $0.4 Z_{\odot}$ ; **light blue:**  $0.2 Z_{\odot}$ ; **dark blue:**  $0.02 Z_{\odot}$ .

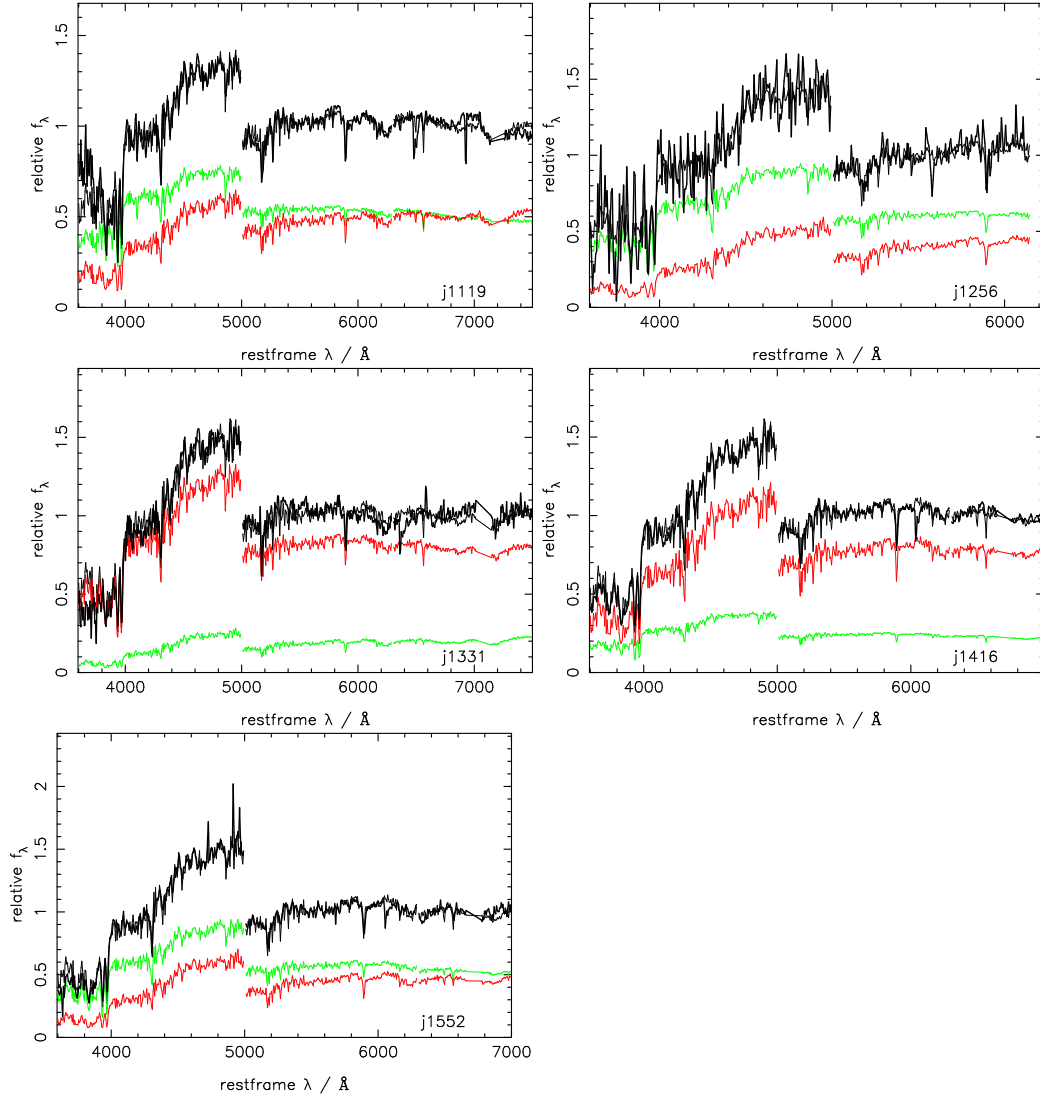


Figure 2: The best-fitting two-component model (thin black line) superimposed over the spectral sections of the fossil galaxies (thick black line). The two component populations are also shown; the dominant population is in red, and the secondary stellar population is in green. The flux normalisation has been arbitrarily adjusted for clarity.

Table 2: Mass-weighted mean values for the best-fitting star-formation history parameters for the fossil and brightest group galaxy samples. The older population is labelled 1, and the younger, 2. The uncertainties quoted are the standard deviations from the mass-weighted mean. Last column shows the mean stellar mass fraction of the older population. The Kolmogorov-Smirnov probabilities that the two samples are drawn from the same populations are also given.

	mean age 1	mean age 2	mean Z1	mean Z2	mass fraction
	Gyr	Gyr	$Z_{\odot}$	$Z_{\odot}$	
<b>BGGs</b>	13.7±0.7	9.8±3.6	2.03±0.68	1.10±0.91	0.79±0.18
<b>fossils</b>	14.0±0.5	10.3±3.4	1.74±0.75	0.33±0.11	0.67±0.19
<b>KS probability</b>	(1-2.4e-7)	(1-6.3e-5)	0.932	0.193	0.871

with wide field camera on Issac Newton Telescope and UIST on UK Infrared Telescope. We perform a similar analysis on the BGG comparison sample, using archival R-band data, observed by the WFI/ESO 2.2m telescope. Table 2 presents the results of the photometric analysis for the two samples.

Most of the non-fossil BGGs (5/6 for which the isophotes were fitted) have boxy isophotes. However, *none* of the fossil BGGs exhibit boxy isophotes [20]. The central fossil galaxies are on average more luminous than the non-fossil BGGs. Given that, in general, more luminous early-types are more likely to have boxy isophotes [29], one would expect that the fossil BGGs would have boxy isophotes if they had evolved in a similar manner to other brightest group or cluster galaxies, but this is not what we see.

The Sersic indices,  $n_S$ , are indistinguishable between the two samples. The mean for both samples is 4.1, and the Kolmogorov-Smirnov probability that the two samples are drawn from the same underlying population is 97 %. However, the fossil galaxies are much larger than the non-fossil BGGs, with a mean half-light radius in the sample  $r_e = 23.1$  kpc, compared with mean  $r_e = 4.6$  kpc for the non-fossil BGGs, and the fossils are on average  $\sim 1$  magnitude brighter than the non-fossils. The Kolmogorov-Smirnov probability that these two samples are drawn from the same underlying population is only 65 %.

## 4 Discussion and Conclusions

We have studied the stellar populations of five central fossil group galaxies using a two-component spectral decomposition of their long-slit optical spectra. Thus, we find the epoch of their last major starburst, and hence their last gas-rich major merger/interaction. We combine this with the photometric analysis, from which we infer the nature of the parent galaxies in the last major merger. We compare these results with those from a control group of seven BGGs, chosen on the basis of the availability of archival data.

We find that i) the dominant stellar components in both galaxy samples are old ( $> 10$  Gyr), metal-rich ( $\geq Z_{\odot}$ ) and statistically indistinguishable in terms of their ages, metallicities and relative mass fractions; ii) the ages of the secondary, younger stellar components are also statistically indistinguishable between the two samples; iii) the central fossil galaxies have secondary stellar components which have significantly lower metallicities than the corresponding stellar populations in the BGG sample; iv) the fossil galaxies have non-boxy isophotal shapes, whereas the non-fossil BGGs are predominantly boxy [20].

Our sample of brightest fossil galaxies is not luminosity-matched to the non-fossil BGG sample; our fossil galaxies are, on average, more luminous than the non-fossils. However,

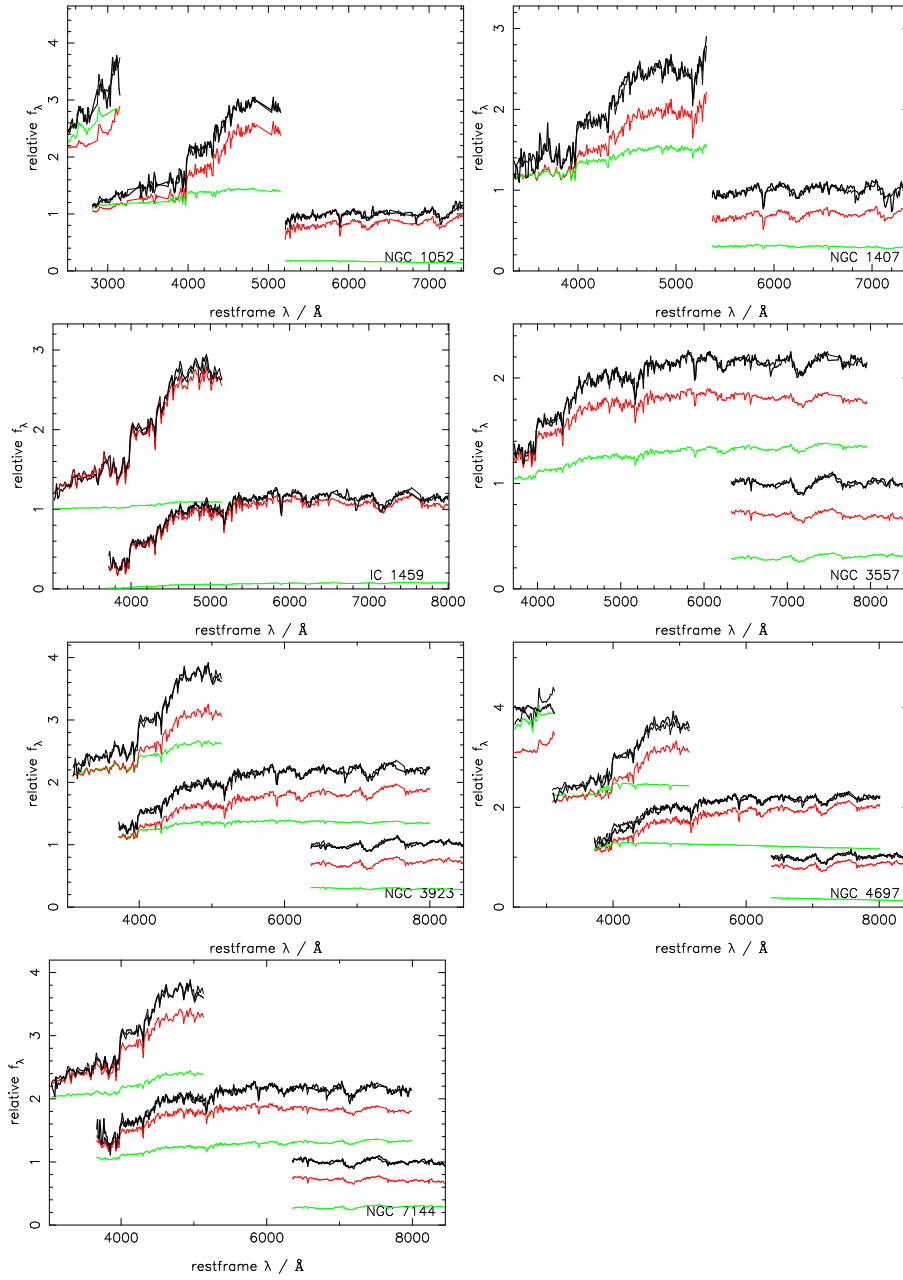


Figure 3: The best-fitting two-component model (thin black line) superimposed over the spectral sections of the brightest group galaxies (thick black line). The two component populations are also shown; the dominant population is in red, and the secondary stellar population is in green. The flux normalisation has been arbitrarily adjusted for clarity.



Table 3: Photometric properties of the sample.

Group	R.A. (J2000)	dec. (J2000)	$z$	$M_R$ mag	$a_4/a$ $\times 100$	$n_S$	$r_e$ kpc
<b>fossil BGGs</b>							
RX J1119.7+2126	11:19:43.6	+21:26:51	0.061	-22.1	0.1	5.1	10.1
RX J1256.0+2556	12:56:03.4	+25:56:48	0.232	-24.1	0.1	3.1	27.2
RX J1331.5+1108	13:31:30.2	+11:08:04	0.081	-22.9	0.3	4.3	11.0
RX J1416.4+2315	14:16:26.9	+23:15:32	0.137	-24.3	0.7	3.6	29.5
RX J1552.2+2013	15:52:12.5	+20:13:32	0.135	-24.0	0.5	4.6	37.9
<b>non-fossil BGGs</b>							
NGC 1052	02:41:04.8	-08:15:21	0.005	-21.6	0.0	4.2	2.12
NGC 1407	03:40:11.9	-18:34:49	0.006	-22.8	-0.3	3.5	4.62
IC 1459	22:57:10.6	-36:27:44	0.006	-22.7	–	3.7	2.95
NGC 3557	11:09:57.6	-37:32:21	0.010	-23.3	-0.2	4.6	10.53
NGC 3923	11:51:01.8	-28:48:22	0.006	-23.0	-0.4	–	–
NGC 4697	12:48:35.9	-05:48:03	0.004	-21.9	1.3	3.8	1.93
NGC 7144	21:52:42.4	-48:15:14	0.006	-21.7	-0.1	5.0	5.54

we expect more luminous galaxies to be *more* metal-rich than lower-luminosity galaxies [21]. Therefore, it seems unlikely that the lower metallicity of the more luminous fossil sample is a simple effect of our luminosity selection. Nor do we expect it to be an effect of the different aperture sizes probing different regions of the two classes of galaxy. Although the sizes of the apertures are different (in kpc), the region from which the spectra are sampled is  $\sim r_e / 5$  in both cases, so the metallicity gradient observed in the cores of early-type galaxies [30] should not be responsible for the significant differences between the metallicities in the young populations. Further, the well-known age-metallicity degeneracy [31] means that the secondary stellar populations in the central fossil galaxies would have to be younger if they were to match the higher metallicities of the corresponding stellar populations in the non-fossil galaxies, and we do not expect any such recent merger-induced major starbursts to be common in the relaxed, symmetrical fossil systems. In any case, the long-baseline spectra contain sufficient data to lift the age-metallicity degeneracy for the dominant populations in early-type galaxies [24].

As described above, we find no difference between the epochs of the last gas-rich merger in our two galaxy samples, but the younger stars in the central fossil galaxies have significantly lower metallicities than those in the non-fossil BGGs. The metallicity of a stellar population created in a starburst due to a major galaxy-galaxy merger or interaction can depend on a number of factors: i) the timescale of the starburst: the longer the duration of a starburst, the more time there is for metals to be created and made available for new stars; ii) how well the metals are retained in the potential well where the starburst is taking place; iii) the initial metallicity of the gas supplied by the parent galaxies; iv) how much un-enriched gas from outer regions is funnelled into the starburst to ‘dilute’ the metal-enrichment occurring in the starburst.

Conventional theory suggests that the later the epoch of formation, the more metal-rich a stellar population must be, as gas becomes increasingly enriched with metals released from earlier generations of stars. Whilst it is true that metals can only exist if earlier stellar generations have pre-existed, we do not in fact observe a simple metallicity-age correlation in the stellar populations of early-type galaxies. In fact, the most metal-rich stellar populations

observed are generally associated with the oldest stellar populations, and we see relatively young stars with significantly lower metallicities [24, 32, 33]. This suggests that metallicity of stars produced in galaxy-galaxy mergers is dependent predominantly on local conditions, and in particular, on the amount of un-enriched gas available to a starburst event. In fact, Kewley et al [34], find evidence that the stronger a central, interaction-induced starburst is, the lower the metallicity of the resulting stellar population. This suggests that in a strong, and therefore gas-rich starburst, un-enriched gas from the outer regions of galaxies is funnelled into the central regions, diluting the pre-existing nuclear gas. As our fossil galaxies are more luminous than the non-fossil BGGs ( $\sim 1$  magnitude), a similar mass fraction in the younger stellar populations represents a more massive starburst in the fossils than in the non-fossil BGGs, consistent with this picture.

The isophotal shapes of early-type galaxies tell us something about the nature of their most recent merger. Recent numerical simulations show that boxy isophotes in early-type galaxies are formed in either equal-mass mergers or gas-poor mergers [6]. Hence, the last major merger / interaction of central fossil galaxies must have been gas-rich, in order to produce their non-boxy isophotes [20]. In this work, we can add to this our knowledge of the detailed star-formation history of the galaxies, which tells us when the last starburst-inducing merger occurred. Of course, in the case of the galaxies with boxy isophotes, the last starburst may not have occurred at the same time as the last major merger. If, as we expect, their last merger was gas-poor, there can have been no significant star-formation in that event. The younger population is therefore likely to be associated with an earlier merging event.

Combining our insights from the photometric and spectroscopic analyses detailed above, we tentatively arrive at the following picture for the formation history of non-fossil BGGs versus that of fossil BGGs, as sketched in Figure 4. Both classes of galaxy formed the bulk of their stars at an early epoch ( $\geq 13$  Gyr ago), and these stars have high metallicities ( $>$  solar metallicity). They then underwent major, gas-rich, star-formation-inducing mergers at time  $t_1$ , represented by the age of the younger stellar population,  $\sim 10$  Gyr. A lookback time of 10 Gyr is a redshift  $\sim 2$ . Reassuringly, this is consistent with the epoch of peak star formation rate (e.g. Heavens et al. [35]), which is presumed to be the peak of merging-induced starbursts. In the fossil BGGs, the merging was very gas-rich, leading to low metallicities in the stars formed. The fossils completed this merging at an early epoch, and have evolved undisturbed since this epoch of merging. The non-fossil BGGs, however, have undergone another round of merging, at time  $t_2$  (which we do not know). As the parent galaxies are now the gas-poor early-type remnants of the previous round of merging, the final product has boxy isophotes, and no further significant star-formation. Hence, we can explain the stellar ages, isophotal shapes and X-ray emission of these two classes of galaxy in a fully consistent manner.

Although of course this study is based on a limited sample of galaxies, we have uncovered some tantalising evidence of differences between the photometric and stellar properties of BGGs and central fossil galaxies, which suggest different formation scenarios for these systems. We intend to follow up our study with a larger, statistically-selected sample, to further probe the statistical differences between star-formation history, luminosity, half-light radius etc. in fossil and non-fossil BGGs. We recognise that the N-body galaxy-galaxy merging simulations discussed here cover a limited parameter space, and we therefore intend to use the upcoming results from new simulations, which will sample a larger parameter space (e.g. mass ratio, orbital characteristics) than previously available, and include cooling, star-formation and black hole growth.

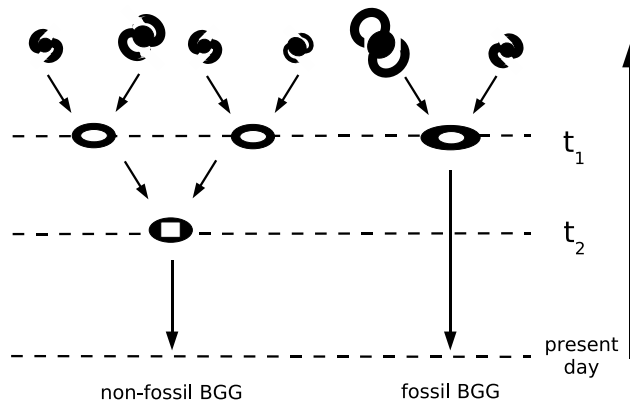


Figure 4: Merger history of fossil BGGs compared with non-fossil BGGs. See §4 for discussion.

## Acknowledgements

This work uses INES data from the IUE satellite. We thank Laurence Jones for his earlier involvement in the spectroscopy of the fossil sample and Patricia Sanchez-Blazquez for discussion on the subject. We thank the anonymous referee for useful comments which improved the presentation of the paper.

## References

- [1] Toomre A., and Toomre J., 1972, *ApJ*, 178, 623
- [2] Barnes J. E., 1988, *ApJ*, 331, 699
- [3] Barnes J. E., Hernquist L., 1992, *ARAA*, 30, 705
- [4] Dubinski J., 1998, *ApJ*, 502, 141
- [5] Naab T., Burkert A., 2003, *ApJ*, 597, 893
- [6] Khochfar S., Burkert A., 2005, *MNRAS*, 359, 1379
- [7] Ponman T. J., Allan, D. J., Jones L. R., Merrifield M., MacHardy I. M., 1994, *Nature*, 369, 462
- [8] Khosroshahi H. G., Ponman T. J., Jones L. R., 2007, *MNRAS*, 377, 595
- [9] Smith G. P., Khosroshahi H. G., Dariush A., Sanderson A. J., Stott J. P., Haines C. P., Egami E., Stark D. P., 2010, *MNRAS*, 409, 169
- [10] Alamo-Martínez K. A., West M. J., Blakeslee J. P., González-Lópezlira R. A., Jordán A., Gregg M., Côté P., Drinkwater M. J., van den Bergh S., 2012, *A&A*, 546A, 15
- [11] Jones L. R., Ponman T. J., Horton A., Babul A., Ebeling H., Burke D. J., 2003, *MNRAS*, 343, 627

- [12] D’Onghia E., Sommer-Larsen J., Romeo A. D., Burkert A., Pedersen K., Portinari L., Rasmussen J., 2005, *ApJ*, 630, 109
- [13] Dariush A., Khosroshahi H. G., Ponman T. J., Pearce F., Raychaudhury S., Hartley W., 2007, *MNRAS*, 382, 433
- [14] Dariush A., Raychaudhury S., Ponman T. J., Khosroshahi H. G., Benson, A. J., Bower R. G., Pearce F., 2010, *MNRAS*, 405, 187
- [15] Mahdavi A., Böhringer H. Geller M. J., Ramella M., 2000, *ApJ*, 534, 114
- [16] Osmond J. P. F., Ponman T. J., 2004, *MNRAS*, 350, 1511
- [17] Rasmussen J., Ponman T. J., Mulchaey J. S., Miles T. A., Raychaudhury S., 2006, *MNRAS*, 373, 653
- [18] Khosroshahi H. G., Maughan B., Ponman T. J., Jones L. R., 2006, *MNRAS*, 369, 1211
- [19] Mendes de Oliveira C. L., Cypriano E. S., Sodré, L. Jr., 2006, *AJ*, 131, 158
- [20] Khosroshahi H. G., Ponman T. J., Jones L. R., 2006, *MNRAS Letters*, 372, 68
- [21] Trager S. C., Faber S. M., Worthey G., Gonzalez, J. Jesús, 2000, *AJ*, 119, 1645
- [22] Terlevich A. I., Forbes D. A., 2002, *MNRAS*, 330, 547
- [23] van Z. L., Barton E. J., Skillman E. D., 2004, *AJ*, 128, 279
- [24] Nolan L. A., Dunlop J. S., Panter B., Jimenez R., Heavens A., Smith G., 2007, *MNRAS*, 375, 371
- [25] Forbes D. A., et al., 2006, *PASA*, 23, 38
- [26] Ellis S. C., O’Sullivan, E., 2006, *MNRAS*, 367, 627
- [27] Bruzual G., Charlot S., 2003, *MNRAS*, 344, 1000
- [28] Nolan L. A., Harva M. O., Kabán A., Raychaudhury S., 2006, *MNRAS*, 366, 321
- [29] Bender R., Surma P., Doebereiner S., Moellenhoff C., Madejsky R., 1989, *A&A*, 217, 35
- [30] Sánchez-Blázquez P., Forbes D. A., Strader J., Brodie J., Proctor R., 2007, *MNRAS*, 377, 759
- [31] Worthey G., 1994, *ApJS*, 95, 107
- [32] Maraston C., Thomas D., 2000, *ApJ*, 541, 126
- [33] Kuntschner H., 2001, *Ap&SS*, 276, 885
- [34] Kewley L. J., Geller M. J., Barton E. J., 2006, *AJ*, 131, 2004
- [35] Heavens A., Panter B., Jimenez R. and Dunlop J., 2004, *Nature*, 428, 625